CHEMISTRY AN ASIAN JOURNAL ACES FULL PAPER

DOI: 10.1002/asia.201201009

Large Two-Photon Absorption of Terpyridine-Based Quadrupolar Derivatives: Towards their Applications in Optical Limiting and Biological Imaging

Tingchao He,[a] Zheng Bang Lim,[b] Lin Ma,[a] Hairong Li,[b] Deepa Rajwar,[b] Yongjun Ying,[a] Ziyun Di,[c] Andrew C. Grimsdale,*[b] and Handong Sun*[a, d]

Abstract: Developing organic chromophores with large two-photon absorption (TPA) in both organic solvents and aqueous media is crucial owing to their applications in solid-state photonic devices and biological imaging. Herein, a series of novel terpyridine-based quadrupolar derivatives have been synthesized. The influences of electron-donating group, type of conjugated bridge, as well as solvent polarity on the molecular TPA properties have been investigated in detail. In contrast to the case in organic solvents, bis-(thienyl)-benzothiadiazole as a rigid conjugated bridge will completely quench molecular two-photon emission in aqueous media. However, the combination of alkylcarbazole as the donor and bis(styryl)benzene as a conjugation bridge can enlarge molecular TPA cross-sections in both organic solvent and aqueous media. The reasonable two-photon emission brightness for the organic nanoparticles of chromophores **3**–**5** in the aqueous media, prepared by the reprecipitation method, enables them to be used as probes for in vivo biological imaging.

Keywords: fluorescence · nonlinear optics · quadrupolar derivatives · terpyridine · two-photon absorption

Introduction

Organic molecules with large two-photon absorption (TPA) cross-sections (δ, expressed in GM = 1×10^{-50} cm^4 s photon^{-1} molecule^{-1}), that can be excited in the range of 700-1000 nm, are of intense interest because of their applications in 3D microfabrication, multiphoton microscopy, upconverted lasing, photodynamic therapy, optical limiting (OL), and bioimaging.[1] These important applications stimulate the design and characterization of organic molecules with large TPA cross-sections or large TPA cross-section per molecular weight values (δM_W^{-1}). The strategies for the design of molecules with large TPA cross-section have been investigated both theoretically and experimentally.[2] The designs include symmetric and asymmetric arrangements, such as the general D–π–D, A–π–A, D–π–A, D–π–A–π–D, and A–π–D–π–A, where D and A denote electron donor and acceptor groups, respectively, and π is a conjugated bridge. The results reveal that the TPA cross-section increases with the electron donating and/or accepting strength, conjugation length, and the planarity of the π-center, whilst the molecules can retain high optical transparency over wide spectral ranges. This is beneficial for applications such as optical limiting, or imaging in absorbing or scattering media such as biological tissues.[1]

It is noteworthy that the aforementioned synthesis strategies are usually effective in organic solvents, but not in aqueous media or the aggregation state. Although many molecules exhibit large TPA cross-sections in organic solvents, most of them are hydrophobic and their photoluminescence (PL) emission suffers from quenching upon aggregation, which seriously limits their applications in solid-state devices and biological imaging. Therefore, there is a need to develop novel materials, which may circumvent the trade-offs and concomitantly provide large TPA in both organic solvents and aqueous media. In the past years, there have been several papers reporting that the aggregation-induced enhancement of TPA behavior is due to the hindering of molecular internal rotation.[3] However, the molecules present negligible TPA properties in organic solvents. Heterocy-

[a] Dr. T. He, L. Ma, Dr. Y. Ying, Prof. H. Sun
Division of Physics and Applied Physics
School of Physical and Mathematical Sciences
Nanyang Technological University, Singapore 637371 (Singapore)
Fax: (+65) 67957981
E-mail: hdsun@ntu.edu.sg

[b] Dr. Z. B. Lim, Dr. H. Li, D. Rajwar, Prof. A. C. Grimsdale
School of Materials Science and Engineering
Nanyang Technological University
Singapore 637371 (Singapore)
E-mail: acgrimsdale@ntu.edu.sg

[c] Dr. Z. Di
Department of Materials
University of Oxford
Parks Road, Oxford OX1 3PN (UK)

[d] Prof. H. Sun
Centre for Disruptive Photonic Technologies
Nanyang Technological University
Singapore 637378 (Singapore)

Supporting information for this article is available on the WWW under http://dx.doi.org/10.1002/asia.201201009.

clic moieties, terpyridines, have been widely used in optoelectronic materials owing to their electron-withdrawing and transporting abilities as well as their special propeller starburst molecular structure.[4] Moreover, due to the starburst moieties of terpyridines that can suppress molecular internal rotation to some extent, large TPA might be expected even in the nanoaggregates. On the other hand, when thiophene, carbazole, and fluorene groups are attached to the central phenylene ring as donors or serve as a rigid π-conjugated center, the molecules can exhibit both strong PL emission and large TPA cross-section.[5] Based on the above considerations, in this study, a series of quadrupolar derivatives **1**–**5** with terpyridines as electron-accepting edge substituents have been synthesized, with the aim to obtain some organic molecules with large TPA in both organic solvents and aqueous media that have promising applications in photonic devices and biological images. Chromophores **1** and **2** are designed to explore the role of the π-bridge, while chromophores **3**–**5** are designed to study the influence of the electron-donating strength on the TPA properties. As a potential application of rationally designed molecules, the optical limiting (OL) behavior for the chromophores has been demonstrated in tetrahydrofuran (THF) solutions. Moreover, the fluorescent organic nanoparticles of the chromophores **3**–**5** prepared by a reprecipitation method[3] show enlarged TPA cross-sections and reasonable two-photon emission brightness, thus strongly indicating their potential application in biological imaging.

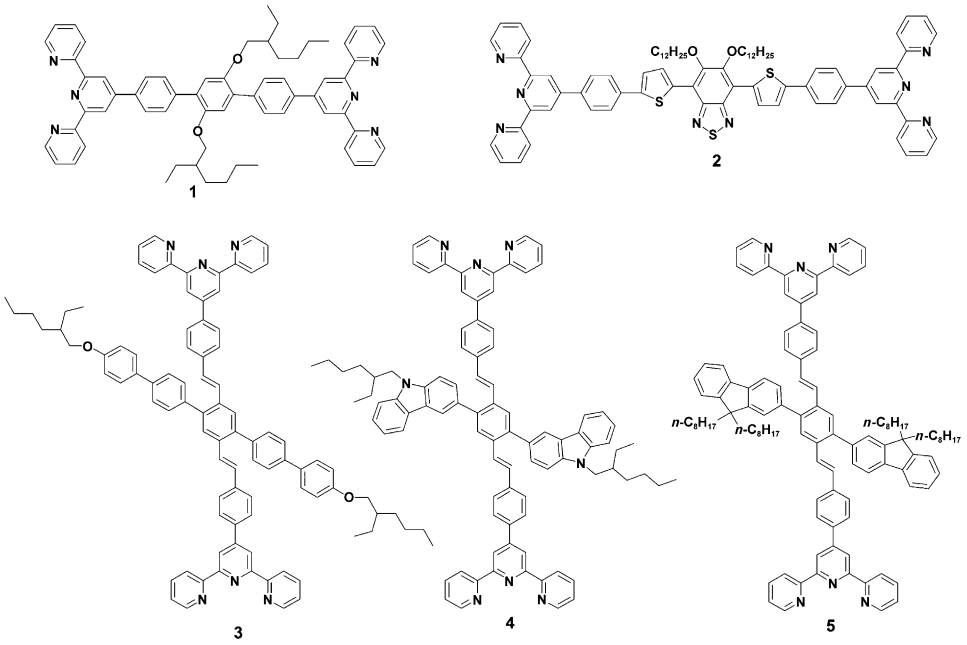

Figure 1. Molecular structures of A-D-π-D-A chromophores studied in this work.

Results and Discussion

The chemical structures of the TPA molecules studied are shown in Figure 1. The synthesis of chromophores **1** and **2** was described in detail in our previous work,[6] while the synthetic procedures of **3**–**5** are described here in the Experimental Section. The molecules presented here have the general structure A–π–A, which differ in the type of conjugation bridge (phenyl in compound **1**, bis(thienyl)-benzothiadiazole in compound **2**, bis(styryl)benzene in compounds **3**–**5**). Alkoxy (**1**, **2**), polyphenylalkoxy (**3**), alkylcarbazole (**4**), and fluorene (**5**) side groups can act as additional donors on the conjugated chain, to form five new quadrupolar-type A–D–π–D–A derivatives.

Linear Optical Absorption and Emission Spectra

Figure 2 shows the UV/Vis linear absorption and PL emission spectra of chromophores in the organic solvents with different polarity: toluene, THF, and chloroform. As shown in Figure 2, a bathochromic shift in the linear absorption spectra was found from **1**→**3**, **5**,→**4**→**2**. This red shift was attributed to the increasing extension of the π-conjugation in the molecules. The order of emission wavelength for chromophores **1**, **3**, **5**, and **4** was consistent with the strength of the donor groups: alkylcarbazole > polyphenylalkoxy > dialkylfluorene > alkoxybenzene. The long emission wavelength of compound **2** arose from its large π-conjugation owing to the rigid planar core structure that consisted of bis(thienyl)- and benzothiadiazole moieties, thereby leading to hindered geometrical (vibrational and rotational) relaxation. Meanwhile, from Figure 2, it can be seen that the linear absorption spectra of chromophores exhibit vibronic structures with progression of several peaks, thus indicating that there is a coupling with vibrational modes in chromophores that correspond to C−C or/and C=C stretching during the excitation from the ground state to the excited state, or the emission from the excited state down to the ground state.[7] The photophysical properties of the molecules in different solvents, including their linear absorption and emission maxima, molar extinction coefficient, and fluorescence quantum yield are also summarized in Table 1. It can thus be concluded that linear absorption maxima and the emission wavelength are red-shifted in solvents with moderate polarity such as in THF, along with a decrease in quantum yield; this indicates that in the excited states these compounds have larger dipole moments relative to their ground state dipole moments.

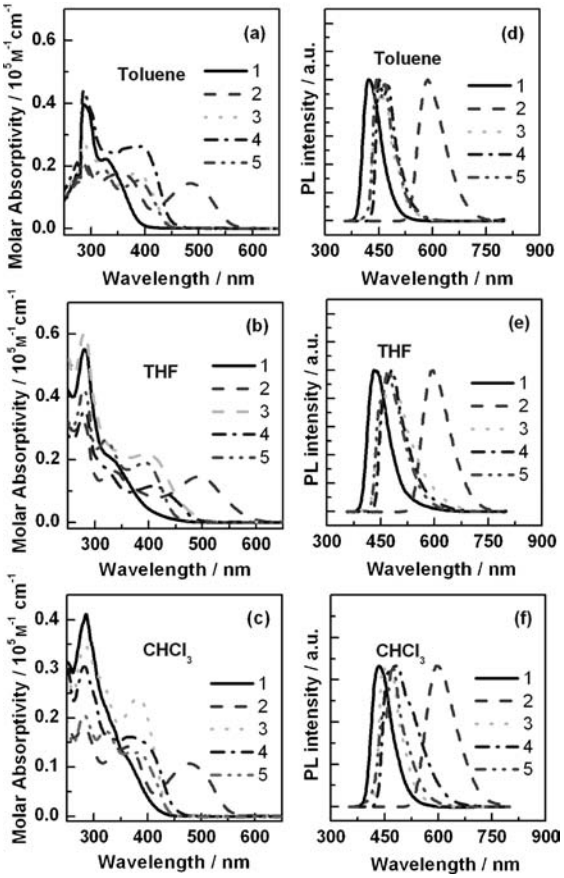

Figure 2. a)–c) UV/Vis absorption spectra of chromophores **1**–**5** in toluene, THF and $CHCl_3$, respectively. d)–f) fluorescence emission spectra of chromophores **1**–**5** in toluene, THF and $CHCl_3$, respectively.

Table 1. Photophysical data of chromophores **1**–**5** in toluene, THF, and $CHCl_3$.

Compound	Solvent	λ_{abs} [nm][a]	ε[b]	λ_{em} [nm][c]	Φ [%][d]	δ [GM][e]	$\delta\Phi$ [GM][f]
	Toluene	328	0.40	423	13	95	12
1	THF	328	0.55	434	11	290	32
	$CHCl_3$	284	0.41	436	20	64	13
	Toluene	483	0.15	586	14	1485	208
2	THF	497	0.15	596	7	4394	308
	$CHCl_3$	478	0.11	597	28	329	92
	Toluene	386	0.18	468	19	624	119
3	THF	412	0.22	474	18	781	141
	$CHCl_3$	383	0.24	469	18	180	32
	Toluene	395	0.26	474	10	2629	263
4	THF	402	0.11	480	8	3826	306
	$CHCl_3$	376	0.16	486	20	643	129
	Toluene	388	0.15	466	20	418	84
5	THF	394	0.19	469	9	794	71
	$CHCl_3$	383	0.13	472	27	121	33

[a] One-photon absorption maxima; [b] Molar extinction coefficient at the absorption maxima given in units of $10^5\,M^{-1}cm^{-1}$; [c] One-photon emission maxima; [d] Fluorescence quantum yield measured at the concentration of 1×10^{-5} M. For chromophores **1**, **3**–**5**, quinine sulfate monohydrate in 0.1 M H_2SO_4 ($\Phi=0.58$) was used as a standard. For chromophore **2**, rhodamine 6G in ethanol ($\Phi=0.95$) was used as a standard. [e] TPA cross-section maxima in the measurable range: 1 GM = 10^{-50} cm^4 s photon^{-1}; [f] TPA action cross-section.

Two-Photon Absorption Spectra

Based on the UV/Vis linear absorption spectra of the chromophores, it is expected that on excitation with femtoscond pulses in the range of 700–900 nm, all the compounds might exhibit TPA behavior. As a matter of fact, two-photon emission could even be observed by the naked eye in chromophores **2**–**5** under the excitation of unfocused laser pulses at 800 nm with a power intensity of several MW cm^{-2}, thereby indicating large TPA action cross-section values. The linear dependence of PL emission intensity on the square of the excitation intensity for the chromophore **2** in THF, as shown in the inset of Figure 3a, confirms that TPA is the main mechanism of strong PL emission. The two-photon emission image for chromophore **2** dissolved in THF irradiated at 800 nm is shown in the inset of Figure 3b, while power intensity dependent two-photon emission spectra and the images for the other four chromophores are given in the Supporting Information (Figure S1–S4). For the chromophores **1**–**5** dissolved in toluene and $CHCl_3$, the two-photon emission intensity versus the square of the excitation power intensity also satisfied the requirements of TPA (see Figures S5–S14 in the Supporting Information). All the chromophores were stable under the experimental conditions and no obvious change was observed in the UV/Vis spectra after the measurements. From the open-aperture *Z*-scan data of chromophore **2**,[8] measured at a concentration of 5×10^{-3} M, as shown in Figure 3b, the TPA cross-section can be determined by fitting to the experimental data. The open-aperture data for the other four chromophores in THF are given in the Supporting Information (Figure S1–S4). To investigate whether or not there was aggregation of ground and/or excited states at the concentrations used to measure TPA, concentration-dependent (in the range between 1×10^{-5} to 1×10^{-3} M) linear absorption measurements were performed. It was found that the observed absorbance was linearly dependent on the concentration of the measured samples, thus indicating that no aggregation of the chromophores took place. Therefore, there was negligible influence of aggregation on the photophysical properties and the measured TPA.

As shown in the TPA spectra presented in Figure 4, compounds **2**–**5**, with the exception of chromophore **1**, display good TPA behavior in the range of 700–800 nm, even if the chromophores are dissolved in nonpolar or polar organic solvents. Moreover, it could be concluded that, as the electron-donating ability increased, the maximum TPA cross-sections (δ_{max}) of chromophores obviously increased. This indicated that the strong TPA activity mainly resulted from large intramolecular charge transfer (ICT). For example, the alkylcarbazole group has stronger electron-donating strength than the polyphenylalkoxy group in compound **3**; the dialkylfluorene in compound **5** and alkoxybenzene in compound **1**, therefore compound **4** showed a higher δ_{max} owing to its stronger ICT effect from

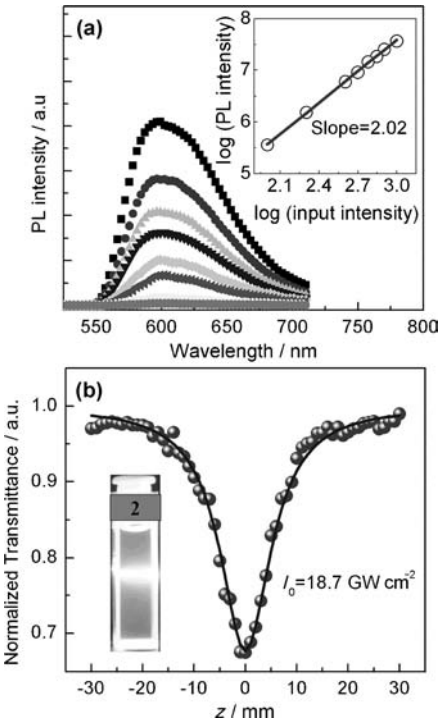

Figure 3. a) Two-photon emission spectra of chromophore **2** in THF under a different power intensity at 710 nm. Inset: the emission intensity versus the square of the excitation power intensity. The log–log plot with a slope value of around 2 indicates the nature of TPA. b) Open aperture *Z*-scan result for chromophore **2** in THF at 710 nm. Scattered dots are the experimental data while the solid line represents the theoretical fitted results. The inset shows the image of two-photon emission for chromophore **2** at 800 nm.

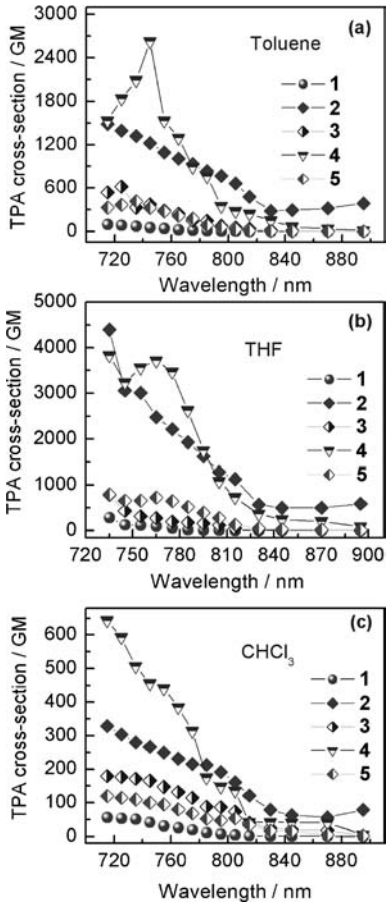

Figure 4. a)–c) TPA spectra of compounds **1**–**5** in toluene, THF, and $CHCl_3$, respectively. The solid lines are provided as a guide.

the middle to the ends of the molecules. Specifically, for the compounds in toluene, compound **4** had a much larger δ_{max} (2629 GM) than compounds **1** (δ_{max} = 95 GM), **3** (δ_{max} = 624 GM), **5** (δ_{max} = 418 GM). Meanwhile, it was noteworthy that compound **2** showed a large TPA cross-section value (δ_{max} = 1485 GM), although the π-conjugated chain was substituted by the alkoxybenzene with weak electron-donating ability. The large δ_{max} of chromophore **2** should be attributed to the high planarity and extended overlap of the π-orbital of bis(thienyl)-benzothiadiazole. Moreover, the Stokes shift of compound **2** (3639 cm^{-1}) was much smaller in comparison to the other chromophores; this further confirmed more intense π-conjugation benefits from structural rigidity of the π-center. This fact clearly showed that careful selection of the π-center and electron-donating group can have a significant impact on the TPA behavior of chromophores in organic solvents.

To assess the potential applications of TPA absorbing molecules, the effect of the molecular environment and solvent polarity should be addressed, as they would affect the intramolecular charge transfer and thus the TPA properties.[9] Hence, we have also investigated the effect of the solvent polarity on TPA cross-sections. Figure 4 a–c shows PA spectra of compounds **1**–**5** in toluene, THF, and $CHCl_3$, respectively. From the data shown in Figure 4, all the chromophores have a much larger δ value in THF, which is of intermediate polarity. It is well known that the solvent polarity can influence the magnitude of intramolecular charge transfer.[10] Compared to toluene and $CHCl_3$, THF can more strongly affect the electronic structure and increase the charge transfer separation in both ground state and excited states; this is expected to be the main reason behind the δ_{max} enhancement.

From the three-state model based on the sum-over-states (SOS) expression, larger M_{ge} (transition dipole moments from ground state to the one-photon-allowed excited state), $M_{ee'}$ (transition dipole moments from the one-photon-allowed excited state to the two-photon-allowed excited state), and smaller detuning energy will result in larger TPA cross-sections.[11] Owing to the limitations of our laser apparatus, we could not obtain the whole TPA spectra to accurately determine M_{ge} and $M_{ee'}$ values. However, M_{ge} can be calculated from the linear absorption spectrum according to the following Equation (1):

$$M_{ge} = \sqrt{\frac{1500(\hbar c)^2 \ln 10}{\pi N_A E_{ge}}} \int \varepsilon_{ge}(\upsilon) d\upsilon \qquad (1)$$

where N_A is Avogadro's number (6.002×10^{23}), $\varepsilon_{ge}(\upsilon)$ is the

extinction coefficient in $cm^{-1}M^{-1}$ as a function of the wavenumber, in cm^{-1}, and the integration is over the main absorption band (all the parameters are in CGS units).[11] For chromophores **1**–**5**, M_{ge} was calculated to be 11.7, 15.9, 13.8, 16.2, and 12.7 D in toluene; 18.3, 21.1, 18.6, 21.1, and 19.2 D in THF; 16.2, 15.8, 17.2, 18.4, 13.7 D in $CHCl_3$, respectively. Apparently, the chromophores **2** and **4** exhibited relatively larger transition dipole moments M_{ge}, which would contribute to the enhancement in their TPA cross-sections.

Two-Photon Absorption Induced Optical Limiting

As the compounds displayed good solubility and large TPA in organic solvents at 710 nm, it allowed us to investigate their OL properties by measuring the relationship between the output intensity and the input intensity, which is one of main applications for two-photon absorbing dyes. For the measurements, the chromophores were dissolved in THF and the concentration was set as 5×10^{-3} M. Due to the relatively poor solubility of chromophore **4** in THF ($<1\times10^{-3}$ M), its OL performance was not included here. The solutions were filled in 1 cm quartz cells. The measured input and output data for these chromophores are plotted in Figure 5a. As shown in the figure, all the compounds showed obvious OL behaviors, especially for compound **2**. When the input fluence increased from 1×10^{-5} to 0.00443 $J\,cm^{-2}$ (443 times increase), the output fluence changed from 1×10^{-5} to 247×10^{-5} $J\,cm^{-2}$ (247 times increase) for compound **1**, from 1×10^{-5} to 64×10^{-5} $J\,cm^{-2}$ (64 times increase) for compound **2**, from 1×10^{-5} to 183×10^{-5} $J\,cm^{-2}$ (183 times increase) for compound **3**, and from 1×10^{-5} to 177×10^{-5} $J\,cm^{-2}$ (177 times increase) for compound **5**. Therefore, if we use the compounds as TPA materials to stabilize the input laser pulse, we would expect that 1.8, 6.9, 2.4, and 2.5 reductions in the laser fluctuation could be achieved for compounds **1**, **2**, **3**, and **5**, respectively. From Figure 5b, the OL thresholds for choromophores **1**, **2**, **3**, and **5**, defined as the input power density at which the transmittance falls to 50% of the linear transmittance, were determined to be >0.00443, 0.00054, 0.00298, and 0.00276 $J\,cm^{-2}$, respectively. The OL performance was superior to many other organic molecules, such as multi-branched styryl derivatives based on 1,3,5-triazine.[12]

Spectroscopic Characteristics of the Nanoparticle Suspensions

Inspired by the high TPA cross-section values of the compounds, we were motivated to examine the PL emission behaviors of their nanoaggregates for application in solid-state devices and biological imaging. The organic nanoparticles were prepared by using a solvent-exchange process, as described in Ref. [13]. For the nanoparticle solutions, the proportion of THF in water was 10% (v/v) and the final dye concentration was 2×10^{-5} M. After mixing, the solution for chromophore **2** remained clear, while for the other four chromophores the solution color changed and the suspension became cloudy. The UV/Vis absorption spectra of chromophores are presented in Figure 6a. As compared to the dyes in THF, except for chromophore **1**, the maximum extinction coefficients for the other four chromophores did not undergo an obvious change. The chromophores **1** and **3** exhibited residual absorption in the longer wavelength, due to the scattering effect of the organic nanoparticles. In addition, the mixture showed stable photophysical properties. No obvious changes in absorption and emission properties were observed after these solutions were stored at room temperature for more than two weeks. With respect to the fluorescence properties, the emission intensity of chromophores **1**–**5** suffered from quenching to different extents (Figure 6b–f). Moreover, the emission peak shifted by 8–32 nm to longer wavelength. The quantum yield of the dye suspensions are listed in Table 2. The dramatic decrease in quantum yield could be ascribed to the increased nonradiative decay of the excited state in the solid state.

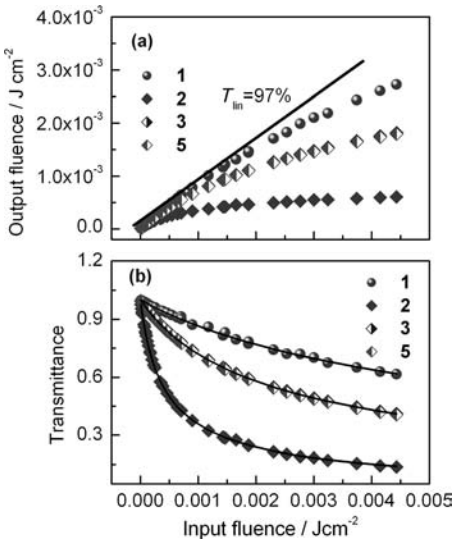

Figure 5. a) Measured output intensity versus input fluence of the 710 nm laser pulse for chromophores **1**, **2**, **3**, and **5** in THF with a concentration of 5×10^{-3} M. b) Transmittance of compounds in THF versus the input fluence. The solid lines represent the best curves with TPA coefficient values of $\beta=0.32\times10^{-10}$ cm W^{-1} (compound **1**), $\beta=4.91\times10^{-10}$ cm W^{-1} (compound **2**), $\beta=0.87\times10^{-10}$ cm W^{-1} (compound **3**), and $\beta=0.89\times10^{-10}$ cm W^{-1} (compound **5**).

It was found that, under the pulse excitation in the range of 700–900 nm, where there was almost no PL emission from chromophores **1** and **2** suspensions, chromophores **3**–**5** exhibited bright PL emission, as shown in the inset of Figure 7. The linear dependence of PL emission versus the square of excitation power intensity indicated the nature of the TPA mechanism (see Figure S15–S17 in the Supporting Information). Although the use of bis(thienyl)-benzothiadiazole as a rigid conjugation bridge could enhance TPA behavior of chromophore **2** in organic solvents, it could not be used in biological imaging because in the suspension the PL emission was completely quenched. The negligible two-photon emission for chromophore **1** should result from its very small intrinsic TPA cross-sections in organic solvents.

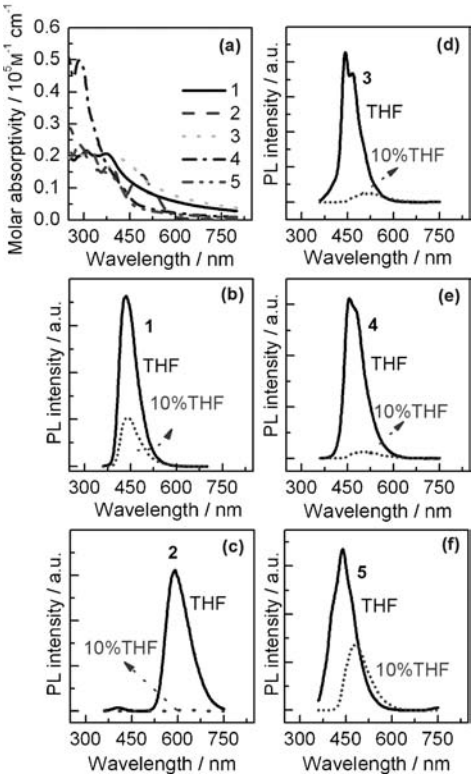

Figure 6. a) Linear absorption spectra of chromophores **1–5** in aqueous media (water/THF mixture, 90% water). b)–f) the comparison of PL emission spectra of chromophores **1–5** in THF and aqueous media under the excitation of 325 nm, respectively.

Table 2. photophysical data of chromophores **1–5** in aqueous media.

Compound	λ_{abs}[a] [nm]	ε[b] [10^5 $M^{-1}cm^{-1}$]	λ_{em}[c] [nm]	Φ [%][d]	δ[e] [GM]	$\delta\Phi$[f] [GM]
1	376	0.21	441	3.1	–	–
2	490	0.14	–	–	–	–
3	447	0.18	518	1.3	1302	17
4	416	0.12	503	0.3	10376	31
5	393	0.14	483	4.0	766	30

[a] One-photon absorption maxima; [b] Molar extinction coefficient at the absorption maxima; [c] One-photon emission maxima; [d] Fluorescence quantum yield. The quinine sulfate monohydrate in 0.1 M H_2SO_4 ($\Phi = 0.58$) was used as a standard; [e] TPA cross-section maxima in the measurable range: 1 GM = 10^{-50} cm^4 s $photon^{-1}$; [f] TPA action cross-section.

An important conclusion can be made here that the appropriate donor donating group and conjugated bridge should be carefully chosen to obtain large TPA properties for application in biological imaging. The introduction of alkylcarbazole as the donor group and bis(styryl)benzene as a conjugated bridge not only enhance molecular TPA behaviors in organic solvents, but also in aqueous media. The TPA spectra of organic nanoparticles for chromophores **3–5**, which were measured by using *Z*-scan technique, are presented in Figure 7. However, there are large error bars (ca. 30%) in the TPA cross-sections, arising from the uncertainties due to scattering influence of nanoparticles. Although their quantum yields decreased, the maximum TPA cross-sections for chromophores **3** and **4** were enhanced by a factor of 1.7 and

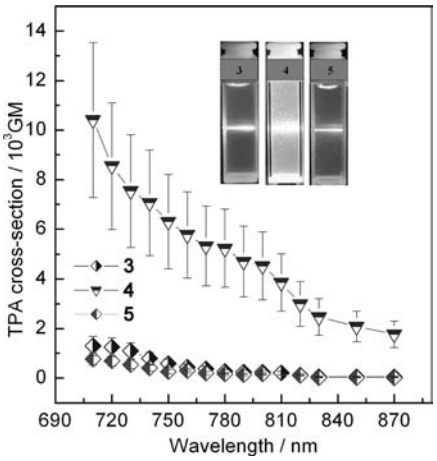

Figure 7. TPA spectra of chromophores **3–5** in aqueous media (water/THF mixture, 90% water) with a total nominal dye concentration of 2×10^{-5} M. Inset: the images of two-photon emission images for chromophores **3–5** in aqueous media at 800 nm.

2.7 times, respectively. Especially, chromophore **4** showed a δ_{max} value of 10376 GM at a concentration of 2×10^{-5} M. This value was extremely high and only a few molecules have shown such high TPA cross-sections, such as porphyrin and squaraine dyes.[14] Owing to intermolecular π–π interactions as well as dipole–dipole interactions between the chromophores in the nanoaggregates, the TPA cross-sections of the molecules could be greatly modified. Moreover, the values could be strongly tuned by the number of molecules and range of relative orientation/distances between interacting chromophores within the organic nanoparticles.[15] Meanwhile, in the aggregates of molecules, bound biexciton states would be formed as a consequence of attractive exciton–exciton interactions, which could result in TPA enhancement. The maximum TPA action cross-sections of chromophores **3–5** were calculated to be 17, 31, and 30 GM, respectively. The decrease of TPA action cross-sections was due to significant reduction in fluorescence quantum yield. Compared to chromophores **3** and **5**, chromophore **4** had a much larger decrease in the maximum TPA action cross-section because of the lower quantum yield. Therefore, the TPA properties of designed molecular structures can be effectively modified. Importantly, although the maximum TPA action cross-sections of organic nanoparticles decreased greatly compared to those in organic solvents, the values were still larger compared to many biocompatible molecules reported previously,[16] strongly suggesting the potential applications of our organic nanoparticles in biological imaging.

Conclusions

The photophysical properties of a series of specifically chosen terpyridine-based TPA molecules have been studied. We have investigated the substantial effects of solvent polar-

ity, electron-donating ability, and the conjugated bridge on their TPA properties. Experimental results clearly indicate that the chromophores exhibit considerably large TPA properties in a moderately polar organic solvent, due to enhanced intramolecular charge transfer. Meanwhile, our experimental results indicate that the magnitude of the molecular TPA cross-section in organic solvents can be effectively enhanced by using strong electron-donating groups or/and rigid π-centers. However, the use of a rigid π-center will result in the complete PL emission quenching of molecules in aqueous media, thereby preventing them from being used in biological imaging. In contrast, the introduction of alkylcarbazole as the donor and bis(styryl)benzene as the conjugation bridge can enhance TPA behavior of chromophores in both organic solvents and aqueous media, thus enabling them to be very promising in solid-state photonic devices and biological imaging.

Experimental Section

*Synthesis of compounds **3**–**5***

The NMR spectra were collected on a Bruker DPX 400 spectrometer using $CDCl_3$ and [D_8]THF as solvents and tetramethylsilane (TMS) as an internal standard. Elemental analysis was obtained on a Thermo Scientific Flash 2000 Series CHNS Analyzer.

Figure 8 shows the molecular structures of chromophores **6**–**9** that were used for the synthesis of chromophores **3**–**5**. The compounds **6**, **7**, and **8** were synthesized according to Ref. [17]. Compound **9** was synthesized by a similar method in Ref. [18]. ^{1}H NMR ([D_8]THF, 400 MHz): δ = 8.80 (s, 2H), 8.67–8.75 (m, 4H), 8.01–8.09 (m, 4H), 7.90 (dd, J = 8.4 Hz, 6H), 7.57 (s, 2H), 7.40 (t, J = 7.2 Hz, 2H), 6.96 (d, J = 15.2 Hz, 2H), 6.78 ppm (d, J = 15.2 Hz, 2H). ^{13}C NMR ([D_8]THF, 101 MHz): δ = 156.7, 156.4, 149.6, 147.9, 138.1, 137.9, 137.2, 136.0, 134.1, 131.0, 130.8, 128.7, 124.8, 122.2, 119.8 ppm. Elemental analysis calcd for $C_{52}H_{34}Br_2N_6$: C: 69.19, H: 3.80, N: 9.31; found: C: 68.94, H: 3.91, N: 9.55.

*Synthesis of compound **3***

Compound **3** was synthesized through coupling compounds **9** and **6.** Compound **9** (0.32 g, 0.36 mmol), **6** (0.26 g, 0.80 mmol), and [$Pd(PPh_3)_4$] (21 mg, 1.80×10^{-2} mmol) were put into a round-bottomed flask and degassed using N_2. Aqueous K_2CO_3 (2.00 M, 10.0 mL) and THF (30.0 mL) were degassed using N_2 and then injected into the flask. The reaction mixture was then stirred in the dark at 80 °C overnight. The reaction mixture was cooled to RT and THF was removed using a rotary evaporator. The reaction mixture was then extracted with CH_2Cl_2 and water. The CH_2Cl_2 layer was dried over $MgSO_4$, concentrated, and the residue mixture was purified by column chromatography on alumina eluting with EtOAc/*n*-hexane (1:9) to afford the product as a yellow solid (0.3 mg, 65.0%). ^{1}H NMR ($CDCl_3$, 400 MHz): δ = 8.77 (s, 4H), 8.73 (d, J = 5.6 Hz, 4H), 8.69 (d, J = 8.0 Hz, 4H), 7.86–7.91 (m, 4H), 7.64–7.72 (m, 6H), 7.57 (d, J = 6.8 Hz, 4H), 7.52 (d, J = 8.4 Hz, 4H), 7.49 (d, J = 4 Hz, 4H), 7.46 (d, J = 4.0 Hz, 4H), 7.43 (d, J = 8.4 Hz, 4H), 7.35 (d, J = 15 Hz, 4H), 7.21 (d, J = 15 Hz, 2H), 3.91 (d, J = 5.6 Hz, 4H), 1.78 (m, 2H), 1.23–1.47 (m, 16H), 0.89–0.94 ppm (m, 12H). ^{13}C NMR ($CDCl_3$, 101 MHz): δ = 156.6, 155.5, 149.6, 148.8, 139.9, 138.4, 137.1, 134.6, 132.8, 132.4, 132.0, 131.9, 130.7, 130.2, 128.7, 128.35, 128.3, 127.5, 127.1, 126.5, 123.8, 121.4, 118.6, 114.8, 68.0, 38.6, 30.3, 28.8, 23.7, 22.8, 14.0, 10.9 ppm. Elemental analysis calcd for $C_{92}H_{84}N_6O_2$: C: 84.63, H: 6.48, N: 6.44; found: C: 84.44, H: 6.56, N: 6.71.

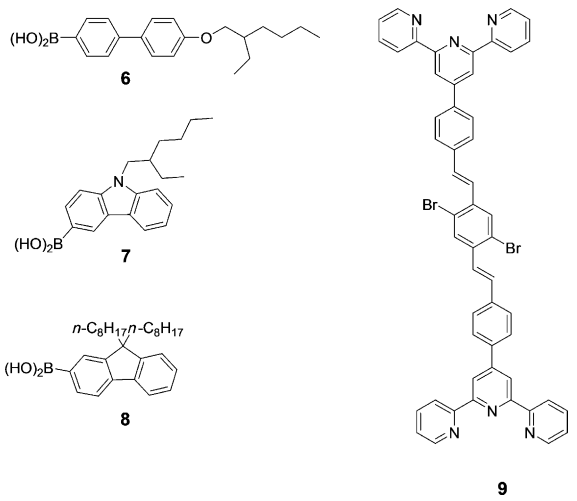

Figure 8. Molecular structures of chromophores **6**–**9** used for the synthesis of chromophores **3**–**5**.

*Synthesis of compound **4***

Compound **4** was synthesized through coupling compounds **9** and **7** by the same method mentioned above. ^{1}H NMR ($CDCl_3$, 400 MHz): δ = 8.74 (s, 4H), 8.71 (d, J = 5.6 Hz, 4H), 8.66 (d, J = 8.0 Hz, 4H), 8.18 (d, J = 7.6 Hz, 4H), 7.83–7.91 (m, 8H), 7.65–7.72 (m, 6H), 7.57 (d, J = 6.8 Hz, 4H), 7.53 (dd, J = 8.4 Hz, 4H), 7.49 (d, J = 4 Hz, 4H), 7.47 (d, J = 7.2 Hz, 2H), 7.41 (d, J = 15 Hz, 2H), 7.33–7.37 (m, 4H), 7.29 (d, J = 15 Hz, 2H), 7.27 (d, J = 7.6 Hz, 2H), 4.22 (d, J = 5.6 Hz, 4H), 1.70 (m, 2H), 1.25–1.47 (m, 16H), 0.88–0.95 ppm (m, 12H). ^{13}C NMR ($CDCl_3$, 101 MHz): δ = 155.5, 154.5, 148.5, 141.3, 140.4, 138.1, 135.2, 133.0, 132.3, 132.0, 130.6, 130.4, 129.3, 129.2, 128.5, 128.3, 128.0, 127.6, 126.5, 123.5, 122.2, 121.2, 119.6, 109.5, 109.0, 47.6, 38.7, 30.3, 28.8, 23.6, 22.8, 13.9. 10.9 ppm. Elemental analysis calcd for $C_{92}H_{82}N_8$: C: 85.02, H: 6.36, N: 8.62; found: C: 84.71, H: 6.49, N: 8.84.

*Synthesis of compound **5***

Compound **5** was synthesized through coupling compounds **9** and **8** by the same method mentioned above. ^{1}H NMR ($CDCl_3$, 400 MHz): δ = 8.79 (s, 4H), 8.76 (d, J = 5.2 Hz, 4H), 8.69 (d, J = 8.0 Hz, 4H), 7.90–7.96 (m, 8H), 7.88 (d, J = 7.6 Hz, 4H), 7.77 (d, J = 7.6 Hz, 4H), 7.75 (s, 2H), 7.63 (d, J = 8.4 Hz, 4H), 7.46 (d, J = 7.2 Hz, 4H), 7.37–7.44 (m, 8H), 7.19 (d, J = 15 Hz, 2H), 2.03 (t, J = 8.4 Hz, 8H), 1.09–1.20 (m, 48H), 0.82 ppm (t, J = 7.2 Hz, 12H). ^{13}C NMR ($CDCl_3$, 101 MHz): δ = 156.2, 155.8, 151.7, 151.3, 149.0, 141.5, 141.4, 141.0, 139.9, 137.9, 136.6, 135.1, 133.6, 131.8, 130.9, 130.8, 130.1, 129.2, 129.0, 128.2, 128.0, 127.8, 127.5, 127.1, 127.0, 125.4, 123.6, 120.4, 120.0, 55.9, 41.0, 32.4, 30.6, 29.88, 29.85, 24.4, 23.2, 14.7 ppm. Elemental analysis calcd for $C_{110}H_{116}N_6$: C: 86.80, H: 7.68, N: 5.52; found: C: 86.59, H: 7.73, N: 5.70.

TPA Cross-Section Measurements

TPA coefficients of molecules were measured using *Z*-scan technique.[8] These compounds were dissolved in organic solvents and placed in 1 mm quartz cells. The laser source was a Ti:Sapphire system that produces 100 fs (HW1/e) pulses at a repetition of 80 MHz. Measurements were carried out in the wavelength range of 700–900 nm for two-photon excitation. In the measurements, the input laser beam was first passed though a beam chopper with an open ratio of 1:10 and a rotating speed of 315 rounds per second. Then the Gaussian beam was tightly focused onto the samples by a convex lens (f = 10 cm). The transmitted beam was detected by a silicon photodiode using the standard lock-in amplifier technique. The measured curves were symmetric with respect to the focal point (z = 0), where they exhibited a minimum transmittance in the case of TPA. The TPA coefficient β can be estimated from the normalized transmittance given by Equation (2):

$$\Delta T = \frac{1}{1+\beta L_{eff}[I_{00}/(1+(z/z_0)^2]} \quad (2)$$

where I_{00} is the peak intensity, z is the sample position, $z_0 = \pi\omega_0^2/\lambda$ is the diffraction length of the beam, ω_0 is the beam waist radius at the focus point, $L_{eff} = [1 - \exp(-\alpha_0 L)]/\alpha_0$ is the effective thickness of the sample. As a macroscopic parameter that depends on the concentration of the TPA molecules, β (in units of cm GW^{-1}) can be further expressed as $\beta = \delta_2^{'} N_0 = \delta_2^{'} N_A d_0 \times 10^{-3}$, where $\delta_2^{'}$ is the molecular TPA cross-section (in units of cm^4 GW^{-1}), N_0 is the molecular density (in units of cm^{-3}), N_A is Avogadro's number, and d_0 is the molar concentration of the absorbing molecules (in units of ML^{-1}). Moreover, one can also use another parallel expression for the TPA cross-section, defined as $\delta = h\nu \cdot \delta_2^{'}$, where $h\nu$ is the photon energy of the input light beam. According to this definition, δ can be calculated in units of GM.[19]

Acknowledgements

The support from the Singapore Ministry of Education through the Academic Research Fund (Tier 1) under Project No. RG63/10 and from the Singapore National Research Foundation through the Competitive Research Programme (CRP) under Project No. NRF-CRP5-2009-04 is gratefully acknowledged. K. C. Wong Foundation is also gratefully acknowledged for Z.D..

[1] a) G. S. He, L. Tan, Q. Zheng, P. N. Prasad, *Chem. Rev.* **2008**, *108*, 1245–1330; b) T. C. He, R. Chen, W. W. Lin, F. Huang, H. D. Sun, *Appl. Phys. Lett.* **2011**, *99*, 081902; c) T. C. He, W. Wei, L. Ma, R. Chen, S. X. Wu, H. Zhang, Y. H. Yang, J. Ma, L. Huang, G. G. Gurzadyan, H. D. Sun, *Small* **2012**, *8*, 2163–2168; d) T. C. He, X. Y. Qi, R. Chen, H. Zhang, H. D. Sun, *ChemPlusChem* **2012**, *77*, 688–693.

[2] a) B. A. Reinhardt, L. L. Brott, S. J. Clarson, A. G. Dillard, J. C. Bhatt, R. Kannan, L. Yuan, G. S. He, P. N. Prasad, *Chem. Mater.* **1998**, *10*, 1863–1874; b) R. Kannan, G. S. He, L. Yuan, F. Xu, P. N. Prasad, A. G. Dombroskie, B. A. Reinhardt, J. W. Baur, R. A. Vaia, L.-S. Tan, *Chem. Mater.* **2001**, *13*, 1896–1904; c) L. Beverina, J. Fu, A. Leclercq, E. Zojer, P. Pacher, S. Barlow, E. W. Van Stryland, D. J. Hagan, J. L. Brédas, S. R. Marder, *J. Am. Chem. Soc.* **2005**, *127*, 7282–7283; d) M. Albota, D. Beljonne, J. L. Brédas, J. E. Ehrlich, J. Y. Fu, A. A. Heikal, S. E. Hess, T. Kogej, M. D. Levin, S. R. Marder, D. McCord-Maughon, J. W. Perry, H. Röckel, M. Rumi, G. Subramaniam, W. W. Webb, X. L. Wu, C. Xu, *Science* **1998**, *281*, 1653–1656; e) D. Beljonne, W. Wenseleers, E. Zojer, Z. Shuai, H. Vogel, S. J. K. Pond, J. W. Perry, S. R. Marder, J. L. Brédas, *Adv. Funct. Mater.* **2002**, *12*, 631–641; f) K. Ogawa, A. Ohashi, Y. Kobuke, K. Kamada, K. Ohta, *J. Am. Chem. Soc.* **2003**, *125*, 13356–13357; g) S. Saito, J. Y. Shin, J. M. Lim, K. S. Kim, D. Kim, A. Osuka, *Angew. Chem.* **2008**, *120*, 9803–9806; *Angew. Chem. Int. Ed.* **2008**, *47*, 9657–9660; h) C. Katan, S. Tretiak, M. H. V. Werts, A. J. Bain, R. J. Marsh, N. Leonczek, N. Nicolaou, E. Badaeva, O. Mongin, M. Blanchard-Desce, *J. Phys. Chem. B* **2007**, *111*, 9468–9483; i) M. Williams-Harry, A. Bhaskar, G. Ramakrishna, T. Goodson III., M. Imamura, A. Mawatari, K. Nakao, H. Enozawa, T. Nishinaga, M. Iyoda, *J. Am. Chem. Soc.* **2008**, *130*, 3252–3253; j) A. Fukazawa, H. Yamada, Y. Sasaki, S. Akiyama, S. Yamaguchi, *Chem. Asian J.* **2010**, *5*, 466–469; k) T. C. He, P. C. Too, R. Chen, S. Chiba, H. D. Sun, *Chem. Asian J.* **2012**, *7*, 2090–2095.

[3] a) B. Wang, Y. Wang, J. Hua, Y. Jiang, J. Huang, S. Qian, H. Tian, *Chem. Eur. J.* **2011**, *17*, 2647–2655; b) Y. Jiang, Y. Wang, J. Hua, J. Tang, B. Li, S. Qian, H. Tian, *Chem. Commun.* **2010**, *46*, 4689–4691; c) W. Qin, D. Ding, J. Liu, W. Z. Yuan, Y. Hu, B. Liu, B. Z. Tang, *Adv. Funct. Mater.* **2012**, *22*, 771–779; d) Y. Hong, J. W. Y. Lam, B. Z. Tang, *Chem. Commun.* **2009**, 4332–4353; e) A. Bhaskar, G. Ramakrishna, K. Hagedorn, O. Varnavski, E. Mena-Osteritz, P. Bäuerle, T. Goodson, *J. Phys. Chem. B* **2007**, *111*, 946–954; f) A. Wild, A. Winter, F. Schlutter, U. S. Schubert, *Chem. Soc. Rev.* **2011**, *40*, 1459–1511.

[4] I. Eryazici, C. N. Moorefield, G. R. Newkome, *Chem. Rev.* **2008**, *108*, 1834–1895.

[5] a) G. L. C. Moura, A. M. Simas, *J. Phys. Chem. C* **2010**, *114*, 6106–6116; b) O. Varnavski, P. Bäuerle, T. Goodson III., *Opt. Lett.* **2007**, *32*, 3083–3085; c) I. Fitilis, M. Fakis, I. Polyzos, V. Giannetas, P. Persephonis, P. Vellis, J. Mikroyannidis, *Chem. Phys. Lett.* **2007**, *447*, 300–304.

[6] Z. B. Lim, H. Li, S. Sun, J. Y. Lek, A. Trewin, Y. M. Lam, A. C. Grimsdale, *J. Mater. Chem.* **2012**, *22*, 6218–6231.

[7] M. Drobizhev, N. S. Makarov, S. E. Tillo, T. E. Hughes, A. Rebane, *J. Phys. Chem. B* **2012**, *116*, 1736–1744.

[8] a) M. Sheik-Bahae, A. A. Said, T. H. Wei, D. J. Haga, E. W. Van Stryland, *IEEE J. Quantum Electron.* **1990**, *26*, 760–769; b) M. Sheik-bahae, A. A. Said, E. W. Van Stryland, *Opt. Lett.* **1989**, *14*, 955–957.

[9] a) H. Y. Woo, B. Liu, B. Kohler, D. Korystov, A. Mikhailovsky, G. C. Bazan, *J. Am. Chem. Soc.* **2005**, *127*, 14721–14729; b) K. Zhao, L. Ferrighi, L. Frediani, C. Wang, *J. Chem. Phys.* **2007**, *126*, 204509; c) M. Johnsen, P. R. Ogilby, *J. Phys. Chem. A* **2008**, *112*, 7831–7839; d) H. Wang, Z. Li, P. Shao, J. Qin, Z. Huang, *J. Phys. Chem. B* **2010**, *114*, 22–27.

[10] C. Reichardt, *Chem. Rev.* **1994**, *94*, 2319–2358.

[11] a) S. Ellinger, K. R. Graham, P. Shi, R. T. Farley, T. T. Steckler, R. N. Brookins, P. Taranekar, J. Mei, L. A. Padilha, T. R. Ensley, H. Hu, S. Webster, D. J. Hagan, E. W. Van Stryland, K. S. Schanze, J. R. Reynolds, *Chem. Mater.* **2011**, *23*, 3805–3817; b) N. Cho, G. Zhou, K. Kamada, R. H. Kim, K. Ohta, S. Jin, K. Müllen, K. Lee, *J. Mater. Chem.* **2012**, *22*, 185–191.

[12] Y. Jiang, Y. Wang, B. Wang, J. Yang, N. He, S. Qian, J. Hua, *Chem. Asian J.* **2011**, *6*, 157–165.

[13] a) J. Luo, Z. Xie, J. W. Y. Lam, L. Cheng, H. Chen, C. Qiu, H. S. Kwok, X. Zhan, Y. Liu, D. Zhu, B. Z. Tang, *Chem. Commun.* **2001**, 1740–1742; b) V. Parthasarathy, S. Fery-Forgues, E. Campioli, G. Recher, F. Terenziani, M. Blanchard-Desce, *Small* **2011**, *7*, 3219–3229.

[14] a) T. K. Ahn, K. S. Kim, D. Y. Kim, S. B. Noh, N. Aratani, C. Ikeda, A. Osuka, D. Kim, *J. Am. Chem. Soc.* **2006**, *128*, 1700–1704; b) H. Rath, J. Sankar, V. PrabhuRaja, T. K. Chandrashekar, A. Nag, D. Goswami, *J. Am. Chem. Soc.* **2005**, *127*, 11608–11609; c) M. Drobizhev, Y. Stepanenko, Y. Dzenis, A. Karotki, A. Rebane, P. N. Taylor, H. L. Anderson, *J. Am. Chem. Soc.* **2004**, *126*, 15352–15353; d) M. Drobizhev, Y. Stepanenko, Y. Dzenis, A. Karotki, A. Rebane, P. N. Taylor, H. L. Anderson, *J. Phys. Chem. B* **2005**, *109*, 7223–7236; e) S. Chung, S. Zheng, T. Odani, L. Beverina, J. Fu, L. A. Padilha, A. Biesso, J. M. Hales, X. Zhan, K. Schmidt, A. Ye, E. Zojer, S. Barlow, D. J. Hagan, E. W. Van Stryland, Y. Yi, Z. Shuai, G. A. Pagani, J. Brédas, J. W. Perry, S. R. Marder, *J. Am. Chem. Soc.* **2006**, *128*, 14444–14445.

[15] a) E. Ishow, A. Brosseau, G. Clavier, K. Nakatani, P. Tauc, C. Fiorini-Debuisschert, S. Neveu, O. Sandre, A. Léaustic, *Chem. Mater.* **2008**, *20*, 6597–6599; b) F. Terenziani, M. Morone, S. Gmouh, M. Blanchard-Desce, *ChemPhysChem* **2006**, *7*, 685–696; c) F. Terenziani, V. Parthasarathy, A. Pla-Quintana, T. Maishal, A.-M. Caminade, J.-P. Majoral, M. Blanchard-Desce, *Angew. Chem.* **2009**, *121*, 8847–8850; *Angew. Chem. Int. Ed.* **2009**, *48*, 8691–8694.

[16] a) A. Kumar, L. Li, A. Chaturvedi, J. Brzostowski, J. Chittigori, S. Pierce, L. A. Samuelson, D. Sandman, J. Kumar, *Appl. Phys. Lett.* **2012**, *100*, 203701; b) S. B. Noh, R. H. Kim, W. J. Kim, S. Kim, K. Lee, N. S. Cho, H. Shim, H. E. Pudavar, P. N. Prasad, *J. Mater. Chem.* **2010**, *20*, 7422–7429; c) P. T. C. So, C. Y. Dong, B. R. Masters, K. M. Berland, *Annu. Rev. Biomed. Eng.* **2000**, *2*, 399–429.

[17] H. Li, S. Valiyaveettil, *Tetrahedron Lett.* **2009**, *50*, 5311–5314.

[18] S. C. Yu, C. C. Kwok, W. K. Chan, C. M. Che, *Adv. Mater.* **2003**, *15*, 1643–1647.

[19] a) G. S. He, G. C. Xu, P. N. Prasad, B. A. Reinhardt, J. C. Bhatt, A. G. Dillard, *Opt. Lett.* **1995**, *20*, 435–437; b) D. Bhawalkar, G. S. He, P. N. Prasad, *Rep. Prog. Phys.* **1996**, *59*, 1041–1070.

Received: October 27, 2012
Published online: December 28, 2012

